

GRAPHOPT: constrained optimization-based parallelization of irregular graphs

Nimish Shah, Wannes Meert, and Marian Verhelst, *Senior Member, IEEE*

Abstract—Sparse, irregular graphs show up in various applications like linear algebra, machine learning, engineering simulations, robotic control, etc. These graphs have a high degree of parallelism, but their execution on parallel threads of modern platforms remains challenging due to the irregular data dependencies. The parallel execution performance can be improved by efficiently partitioning the graphs such that the communication and thread synchronization overheads are minimized without hurting the utilization of the threads. To achieve this, this paper proposes GRAPHOPT, a tool that models the graph parallelization as a constrained optimization problem and uses the open Google OR-Tools solver to find good partitions. Several scalability techniques are developed to handle large real-world graphs with millions of nodes and edges. Extensive experiments are performed on the graphs of sparse matrix triangular solves (linear algebra) and sum-product networks (machine learning). GRAPHOPT achieves an average speedup of $1.4\times$ and $6.1\times$ over the Intel Math Kernel Library and a commonly-used heuristic partitioning technique, respectively, demonstrating the effectiveness of the constrained optimization-based graph parallelization.

Index Terms—graph parallelization, partitioning, constrained optimization, sparse matrix triangular solves, sum-product networks

1 INTRODUCTION

SIGNIFICANT advances have been made in accelerating massively parallel computations like image processing and deep neural networks, which typically involve *regular* memory accesses and well-structured explicit parallelism. These advances can be ascribed to dedicated programming frameworks like Tensorflow [1] and Halide [2], optimized compilation approaches like polyhedral compilation [3], and specialized hardware architectures like GPU and TPU. However, these approaches cannot be readily extended to another equally important class of parallel applications that is *irregular*. Such applications involve irregular memory accesses lacking any apparent recurring patterns, and parallelism that is difficult to partition. Such computations arise in applications like graph workloads, sparse linear algebra, probabilistic machine learning, recommender systems etc.

A subset of these irregular applications can be represented as static directed acyclic graphs (DAG), where the nodes represent operations to perform and edges represent data dependencies among these operations. These DAG workloads can be further classified into two categories: 1) coarse-grained and 2) fine-grained, as shown in fig. 1. The coarse-grained DAGs, although irregular, have as their nodes large regular operations like dense tensor operations. The computation within each node is enough to amortize parallelization costs associated with thread synchronization, inter-thread communication, GPU kernel launch, etc. The examples of coarse-grained graphs include neural networks and linear algebra with block/structured sparsity, graph neural networks, visual rendering, electronic circuit placement, video encoding etc. These applications can be acceler-

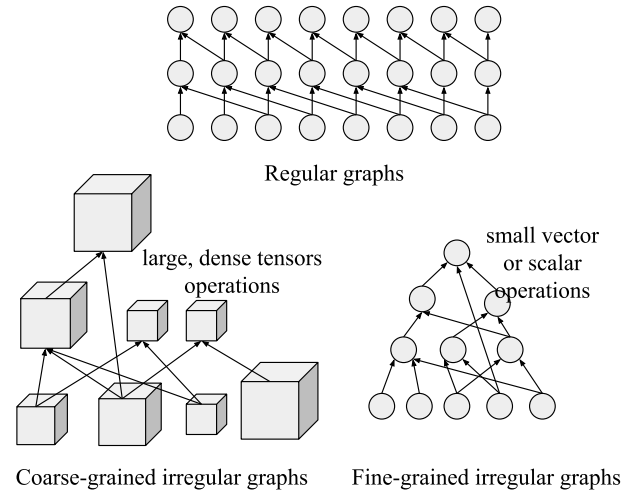


Fig. 1. Illustration of regular, coarse-grained irregular and fine-grained irregular compute graphs

ated efficiently using frameworks like Tensorflow, TaskFlow [4], Intel Thread Building Blocks (TBB) [5] and others [6], [7], by modeling nodes as individual tasks.

On the other hand, the nodes in fine-grained DAGs represent only a couple of scalar operations, whose computation cost cannot amortize synchronization and task launch overheads when each node is modeled as an individual task. As a result, these DAGs cannot be accelerated by simply modeling them as task graphs in Tensorflow, etc. Their acceleration needs the creation of coarser partitions by combining original fine-grained nodes, to increase computation to synchronization/communication ratio. But if the partitions become *too* coarse, they hurt parallelism as there might not be enough partitions to execute in parallel. Hence, appropriate granularity and parallelism of the partitions are

- N. Shah and M. Verhelst are with the Department of Electrical Engineering - MICAS, KU Leuven, Belgium.
- W. Meert is with the Department of Computer Science - DTAI, KU Leuven, Belgium.

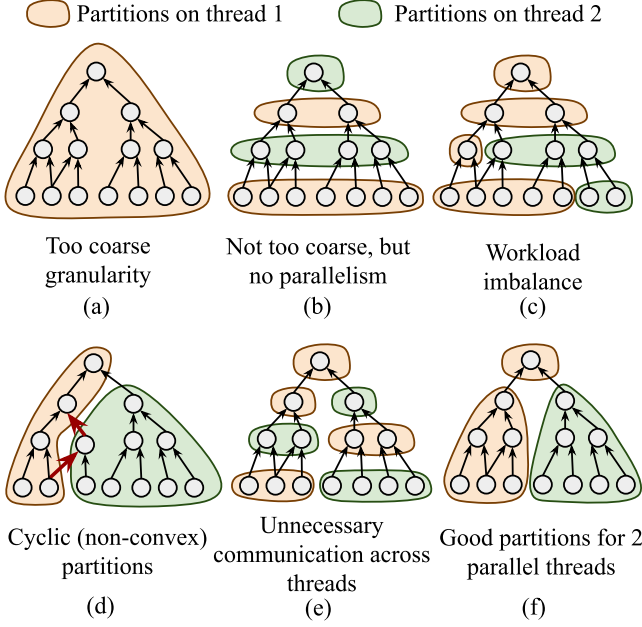


Fig. 2. Different ways to partition a DAG, and impact on parallelization, communication, and workload balance

critical for good acceleration. To this end, this paper proposes **GRAPHOPT**¹—a partitioner to efficiently parallelize fine-grained DAGs through hardware-aware partitioning. The key contributions of the paper are as follows:

- GRAPHOPT models the graph partitioning for parallel execution as a constrained optimization problem, and leverages a state-of-the-art solver to find good partitions.
- Several scalability techniques are proposed to handle real-world graphs with millions of nodes and edges.
- The performance of GRAPHOPT is validated for two applications: 1) sparse matrix triangular solves from linear algebra and 2) sum-product networks from machine learning, and compared against standard libraries.

The paper is organized as follows. Section 2 defines the problem of parallelizing fine-grained DAGs and GRAPHOPT’s approach. Section 3 details the working of GRAPHOPT, followed with extensive performance benchmarking in section 4. Finally, section 5 discusses related works and section 6 concludes the paper.

2 GRAPH PARTITIONING FOR PARALLELIZATION

Modern computing platforms like multi-core CPUs and GPUs are equipped with parallel hardware threads, which can execute DAG nodes in parallel. However, the nodes cannot be arbitrarily scheduled because of the data dependencies represented by the DAG edges, i.e., a node can only be executed after all the *predecessor* nodes have finished their execution. This data dependency demands threads synchronization when a predecessor node is mapped to a different thread than the current one. Furthermore, the nodes in raw fine-grained DAGs do not have enough computation to be executed as a stand-alone

task in a task-scheduling framework (like Intel TBB [5], etc.) because of the task-launch and synchronization overheads. This can be addressed by clustering the nodes in *coarser partitions* that are executed as monolithic tasks to amortize the overheads. The quality and correctness of these coarser partitions depend on several aspects as discussed next (with illustrations in fig. 2).

Data dependencies and acyclic partitions: The data dependencies of DAG edges imply that a partition can be launched as a monolithic unit only if all the predecessor partitions have finished the execution. Furthermore, the edges between partitions should not create cycles, because cyclic partitions need intermittent synchronization with other partitions to resolve intermediate data dependencies. The cycles can be prevented by generating *convex* partitions, i.e., if two nodes are in a partition, the nodes on all the (directed) paths in between the two nodes also have to be in the partition. An example of cyclic partitions is shown in the fig. 2(d). GRAPHOPT avoids these cycles by enforcing an acyclic constraint.

Granularity and parallelism: The sizes of the partitions dictate how often the threads need to synchronize and communicate. To reduce the overall runtime, there are multiple, conflicting, requirements:

- Partitions should be as large as possible to amortize the overheads and increase the local data reuse, minimizing communication across threads. Eg., increasing the granularity in fig. 2(c) and (e) helps.
- There should be enough parallel partitions to keep all the available threads in the underlying hardware busy. Partitions in fig. 2(a) and (b) do not have any parallelism across threads at all.
- Partitions that are supposed to execute in parallel should be of similar size to balance the workload across threads. Figure 2(c) shows a counter-example.

These requirements suggest that the partition granularity depends on the parallelism of the underlying hardware like the number of CPU threads, which is fixed and known beforehand. It also depends on the available parallelism in the DAG, which can vary in the different parts of the DAG. Hence, the partition granularity cannot be manually fixed but has to be automatically adjusted depending on the DAG structure. GRAPHOPT achieves a balance by generating partitions that are as large as possible, as long as there are enough parallel partitions.

Communication: An edge from one partition to the other indicates communication of data. If the two partitions are executed on the same thread, the data can be locally reused via local caches or scratchpads. Whereas, the communication across threads incurs a higher overhead of flushing data to the shared caches. This communication overhead can be reduced by keeping the edges within the same thread as much as possible. Figure 2(e) shows an example where partitions can be simply remapped to different threads to avoid inter-thread communication.

GRAPHOPT’s approach: To appropriately handle the

1. To be open-sourced

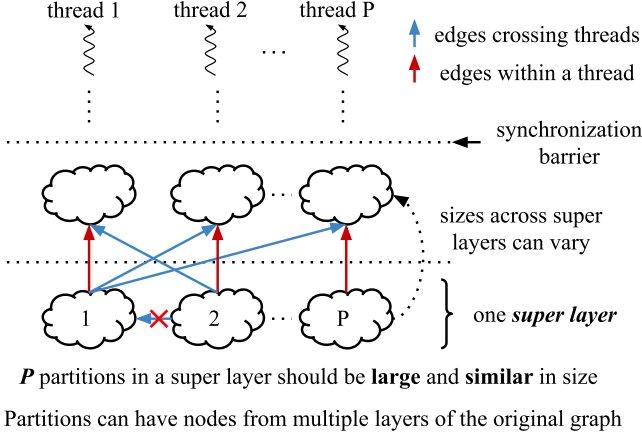


Fig. 3. GRAPHOPT decomposes a fine-grained DAG into *super layers*, each having P partitions. The partitions are made as large as possible but also of similar size to ensure workload balancing

various trade-offs, instead of creating arbitrary partitions, GRAPHOPT creates a layered graph of coarse partitions as shown in fig. 3. To avoid confusion, a layer of coarse partitions is always referred to as a *super layer* in the rest of the paper, and a *layer* simply means a layer of nodes in the original fine-grained DAG. Every super layer has P independent partitions, where the user can specify an arbitrary P based on the target hardware (e.g. P can be set to 8 for a CPU with 8 single-threaded cores). This ensures that, whenever possible, all the P hardware threads have a corresponding partition to execute. The partitions in a super layer are independent, i.e. there is no edge crossing among them, enabling parallel execution. The parallel threads need to be synchronized after every super layer to allow race-free data communication needed by the blue edges. GRAPHOPT models this multi-objective problem of DAG partitioning to create super layers as a constrained optimization problem, as explained in the next section.

3 GRAPHOPT

This section explains the generation of super layers with P parallel balanced coarse partitions from a fine-grained DAG. The optimal graph partitioning, even without the acyclic constraint and parallelism requirement, is known to be NP-complete [8], [9]. Recent work [10] has shown that graph partitioning with the acyclic constraint is also NP-complete. Section 5 explains why general graph partitioning approaches cannot be used here because of the parallelism requirement (P independent partitions) and the acyclic constraint. These general approaches only focus on minimizing edges among (possibly cyclic) partitions, and do not aim to generate layered graphs with P parallel workload-balanced partitions needed to keep parallel threads busy.

Figure 4 shows GRAPHOPT's approach for generating partitioned super layers. To reduce the complexity, instead of finding all the super layers simultaneously, the tool iteratively constructs one super layer at a time going from the bottom to the top. In an iteration, a super layer is generated with two main steps: (M1) recursive two-way partitioning and (M2) workload-balancing. The S1, S2, and

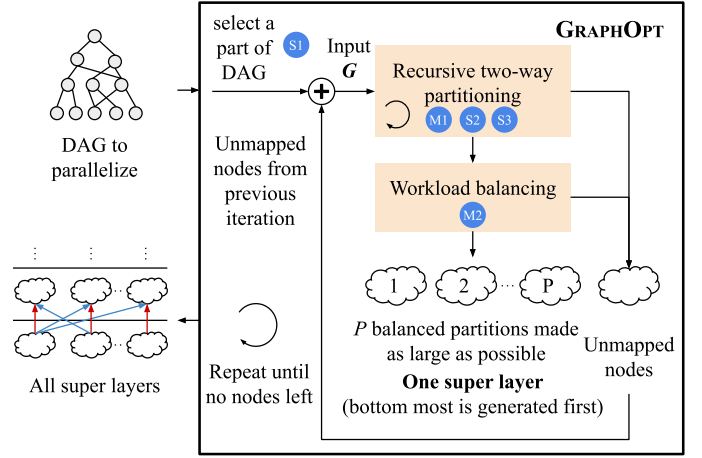


Fig. 4. The overview of the iterative algorithm of GRAPHOPT. One super layer, starting from the bottom, is generated in every iteration. The main steps M1 and M2 use an optimization model with the Google OR-tool solver [11] to find good partitions. The scalability steps S1, S2, and S3 are used to handle graphs with millions of nodes/edges.

S3 are the scalability techniques that enable GRAPHOPT to handle large graphs with millions of nodes/edges.

An iteration starts by selecting a part of the DAG that is considered for generating the current super layer. Ideally, all the currently unmapped nodes should be considered, but to limit the complexity, the step S1 selects a subgraph G from the unmapped DAG. The M1 step splits this subgraph G into P parallel partitions and associates them to the P underlying hardware threads. These partitions, however, could potentially be of different sizes. The M2 step redistributes nodes among these partitions for workload balancing, generating P balanced partitions for the current super layer. The unmapped nodes that could not be mapped to any partitions are then considered for the subsequent super layers.

3.1 Recursive two-way partitioning (M1)

Given a subgraph G , a super layer with parallel partitions should ideally be constructed by a direct P -way partitioning. GRAPHOPT relaxes this by using recursive *two-way* partitioning, i.e. recursively splitting subgraphs into two parallel smaller subgraphs until getting P subgraphs (partitions) for P threads, as illustrated in fig. 5(top). The recursion starts with the aim of mapping the input subgraph G to P threads. The first two-way partition generates two output partitions, one of which represents the nodes corresponding to $t_1, \dots, t_{P/2}$ threads, and the other corresponding to $t_{P/2+1}, \dots, t_P$ threads. The third output is a set of unmapped nodes that cannot be mapped to either partition without adding an edge between the partitions. These unmapped nodes will be considered for the subsequent super layers. The next recursion splits the first partition (which becomes the current G) into two smaller partitions, one for $t_1, \dots, t_{P/4}$ threads and the other for $t_{P/4+1}, \dots, t_{P/2}$ threads. This repeats until partitions for individual threads are determined. Thus the problem of one super layer generation is reduced to multiple iterations of two-way partitioning under given constraints and objectives. Note that if P is not a power of 2, the partitions can end up being imbalanced, which is addressed with the M2 step.

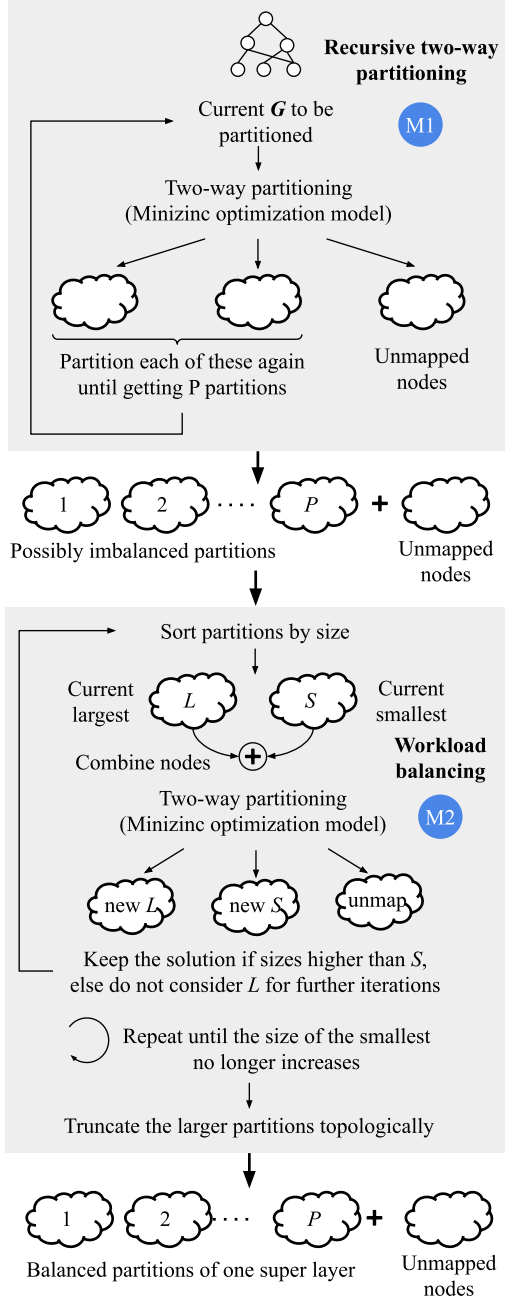


Fig. 5. The recursive two-way partitioning (M1) uses a Minizinc-based optimization model to partition subgraphs until getting P partitions. Due to the recursive approach, the partitions can be imbalanced. The workload balancing (M2) iteratively redistributes the nodes, using the same Minizinc-based model, to generate a balanced super layer

Instead of developing a custom heuristic algorithm, GRAPHOPT models the two-way partitioning problem with the Minizinc constrained-optimization language [12]. Such a model can be solved with state-of-the-art constraint programming (CP) or mixed-integer linear programming (MILP) solvers like Google OR-Tools [11], SCIP [13], Gurobi [14] etc. These solvers are designed and tuned with decades of research and often outperform custom heuristics for smaller problem instances, but struggle to scale to larger problems. This is addressed in this work by developing the scalability techniques explained later in sec. 3.3. An

optimization model consists of four parts: 1) inputs of the problem, 2) decision variables whose values need to be determined by the solver, 3) constraints on the decision variables, and 4) the objective of the optimization (refer [15] for more details of constrained optimization). The rest of the section describes these four parts.

3.1.1 Optimization model for the two-way partitioning

Given an input graph, the two-way partitioning aims to allocate the nodes to two parallel partitions such that there is no edge crossing from one to the other. Furthermore, the size of the partitions should be as large and equal as possible. If the target for the current recursion are t_1, t_2, \dots, t_x threads, the first output partition corresponds to $t_1, \dots, t_{x/2}$ threads and other to $t_{x/2+1}, \dots, t_x$ threads. The inter-thread communication (blue edges in fig. 3) would reduce if the sources of the incoming edges of the partitions are from the same group of threads. Hence, one of the aims of the two-way partitioning is also to perform allocation such that the nodes in the first partition mostly have incoming edges from $t_1, \dots, t_{x/2}$ threads, and the second partition from $t_{x/2+1}, \dots, t_x$ threads.

Table 1 shows the inputs and the decision variables of this problem. The current input DAG is denoted by $G(V, E)$, where V is the set of nodes (vertices), and E is the set of directed edges. Note that this is not the complete original DAG, but an input subgraph for the current recursion of the two-way partitioning. The output partitions of G are decided by the decision variable $PART(V)$, an array of integers, one for every node. If $PART[v] = 1$ or 2 , the node v is allocated to the partition 1 or 2 respectively, and if $PART[v] = 0$, it is not allocated. The other inputs and decision variables are discussed next along with the related constraints and objective.

Acyclic and data-dependency constraint

There should not be any edge from one partition to the other, which implies that, for the destination and source nodes of every edge, $PART[dst]$ should either be equal to $PART[src]$ or should be 0. This also ensures that the destination node is unallocated if the source node is also unallocated, which is needed because the edges represent data-dependencies. This constraint is modelled as follows (the \vee symbol indicates the logical or operation),

$$\forall (src, dst) \in E, \\ PART[dst] = PART[src] \vee PART[dst] = 0 \quad (1)$$

Partition size constraint

The input parameter $node_w(V)$ (array of integers) represents the amount of computation to be performed in each node. For workload balancing, the amount of computation in the two partitions should be the same. To formulate such an optimization objective, the decision variables $PART_1_size$ and $PART_2_size$ are used, which are modelled with the following constraint,

$$\forall v \in V, \\ PART_1_size = \text{sum}(node_w[v] \mid \text{if } PART[v] = 1) \\ PART_2_size = \text{sum}(node_w[v] \mid \text{if } PART[v] = 2) \quad (2)$$

TABLE 1
Inputs and decision variables for the Minizinc two-way partitioning optimization model

| Name | Description | Type |
|---|--|-----------------------|
| Inputs | | |
| t_1, \dots, t_x | Target threads for this recursion | array of int |
| V | Set of nodes in the current DAG G | set of int |
| $E(V, V)$ | Set of directed edges in G expressed as tuples of source and destination nodes | set of int tuples |
| $node_w(V)$ | Weights indicating the amount of computation within nodes | array of int |
| V_{in} | Set of nodes that are already allocated to previous super layers | set of int |
| $E_{in}(V_{in}, V)$ | Set of directed edges with source node in V_{in} and destination in V | set of int tuples |
| $PART_{in}(V_{in})$ | Allocated partitions of nodes in V_{in} | array of int in [1,2] |
| Decision variables: Final output | | |
| $PART(V)$ | Allocated partitions for nodes in V , where 0 indicates no allocation | array of int in [0,2] |
| Decision variables: Intermediate | | |
| $PART_1_size$ | Amount of computation allocated to partition 1 | int |
| $PART_2_size$ | Amount of computation allocated to partition 2 | int |
| $E_{in_crossing}(E_{in})$ | Indicates whether the edge in E_{in} are crossing partitions or not | array of bool |

Inter-thread communication constraint

The blue edges in fig. 3 contribute to inter-thread communication. An edge would become a blue edge if its source node is already allocated in a previous super layer to a thread t_a , and the destination node is currently allocated to a partition that does not correspond to t_a . Note that these edges are not in the current edge set E , because the edges in E have the source and destination nodes that are being considered for the current super layer. Another input to the model E_{in} represents such edges, which have source nodes (represented by the set V_{in}) in the previously generated super layers, and destination nodes in the current G . Input $PART_{in}(V)$ represents the partitions of the nodes in V_{in} based on the threads they are allocated to. If a v_{in} was allocated to any of the threads $t_1, \dots, t_{x/2}$ in the previous super layers, $PART_{in}[v_{in}] = 1$, and if allocated to any of the $t_{x/2+1}, \dots, t_x$ threads $PART_{in}[v_{in}] = 2$. If a v_{in} was not allocated to any of the current target threads t_1, \dots, t_x , its corresponding edges always result in inter-thread communication irrespective of how the current partitioning is done. Hence, such v_{in} and the corresponding edges are not considered in the model.

An edge in E_{in} is a *crossing* edge when the partitions of the destination and source nodes are different. The edge crossings are tracked with $E_{in_crossing}$ (array of booleans), modeled with the following constraint,

$$\forall(src, dst) = e \in E_{in}, E_{in_crossing}[e] = ((PART[dst] \neq 0) \wedge (PART[dst] \neq PART_{in}[src])) \quad (3)$$

The first inequality makes sure that the edges with unallocated destination nodes are not marked as crossing edges. The \wedge symbol indicates the logical *and* operation.

Objective

The objectives of GRAPHOPT are maximizing but also equalizing the partition sizes and minimizing the edge crossings. The optimization solvers generally support only one objective, hence a weighted sum of the multiple objectives is used. The objective makes sure the smaller of the two partitions is made as big as possible.

$$\begin{aligned} &\text{maximize } w_s \times \min(PART_1_size, PART_2_size) \\ &\quad - w_c \times \text{sum}(E_{in_crossing}) \end{aligned} \quad (4)$$

In our experiments, w_s is kept $10 \times w_c$. The objective along with the constraints in the equations 1-4 form the Minizinc

optimization model for the two-way partitioning problem, which is solved with the Google OR-Tools solver.

3.1.2 Example

The figure 6 illustrates the optimal two-way partitioning of a simple G . The nodes set V is $\{1, \dots, 9\}$ and the edge set E is $\{(1,5), (2,5), \dots, (8,9)\}$. The computation in every node, the $node_w$, is assumed to be 1. Assume that the target threads are $\{t_1, \dots, t_4\}$. The incoming edges E_{in} are $\{(10,1), (10,7), \dots, (13,4)\}$ and suppose their source nodes V_{in} , $\{10, \dots, 13\}$, are mapped to the threads $\{t_2, t_2, t_4, t_3\}$ respectively, in the previous super layers. Hence, $PART_{in}[10] = PART_{in}[11] = 1$, and $PART_{in}[12] = PART_{in}[13] = 2$.

The variable $PART[9]$ for the top node will remain 0, otherwise due to the constraint in the eq. 1, all the nodes would end up in the same partition (which would be a valid but suboptimal solution). The $PART$ for the other nodes are decided such that the $E_{in_crossing}$ (blue edges) are minimized. Switching the $PART$ of 1,2,5,7 with 3,4,6,8 would lead to more blue edges. Hence, the solution shown in the figure is the optimal solution. In one of the next recursions, G will contain $\{1,2,5,7\}$ nodes with the target threads $\{t_1, t_2\}$. And the other recursion will be with $\{3,4,6,8\}$ nodes and target threads $\{t_3, t_4\}$. Node 9 is an unmapped node, which will return to the set of remaining nodes to be used in the construction of the next super layer.

3.2 Workload balancing (M2)

A penalty of using recursive two-way partitioning instead of a direct P -way partitioning is that the P partitions are not guaranteed to have the same size. The two-way partitioning attempts to equalize the partition sizes, but this does not guarantee equal parallelism. This imbalance can lead to divergences in partition sizes in subsequent recursions. Moreover, the imbalance can also occur when P is not a power of 2. To address this, a workload balancing step (M2) is used as shown in fig. 5(bottom), which redistributes the nodes across imbalanced partitions. In every iteration, the partitions are sorted according to the sizes. The nodes of the largest and the smallest partitions are combined and two-way repartitioned (with the Minizinc model) in an attempt to redistribute the workload. This repeats until the size of the smallest no longer increases further. If the sizes are still

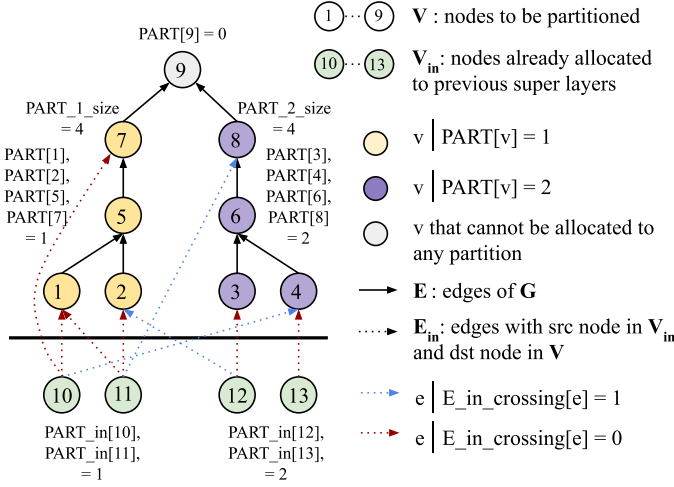


Fig. 6. An optimal solution of the optimization model for a simple graph

unequal, the larger partitions are truncated in topological order to equalize the sizes (with some margin). The truncated nodes will be added to the pool of unmapped nodes to be considered for the next super layer. The final output of this step is a super layer with balanced P partitions.

3.3 Scale to large graphs (S1, S2, S3)

The two-way partitioning model can handle graphs with tens of thousands of nodes and edges in a reasonable time. Hence, the M1 and M2 steps explained earlier are sufficient to generate super layers for such graphs. However, graphs from real applications can have millions of nodes/edges, making the solver runtime prohibitively long. GRAPHOPT uses several techniques to handle the complexity of such large graphs, as shown in the full flow in fig. 7.

Consider limited layers (S1)

Ideally, all the unmapped nodes of the DAG should be considered for allocation in every iteration of super layer generation. However, during the partitioning for initial *bottom* super layers, it is unlikely that the nodes from the *top* of the graph will be allocated. Hence, it is wasteful to consider the entire unmapped graph for the partitioning, and the complexity can be limited by choosing a subset G . With this aim, each node in the graph is assigned to a layer number before beginning the generation of super layers, using the “as last as possible” heuristic, such that every node is in one layer below its lowest successor node. In every iteration, GRAPHOPT adaptively considers a limited number of layers of the unmapped graph, chosen such that the input graph G for the M1 step has a size α (set to 4 in our experiments) times the size of the output super layer in the previous iteration. This automatically chooses an appropriate sized G depending on the parallelism in the DAG. A high α leads to better super layer quality at the expense of partition time, and vice-versa.

Independent connected components (S2)

During the recursive two-way partitioning (M1) (and also M2), the current G to partition may not be a fully connected graph, but may have multiple disconnected components.

This can simplify the partitioning because disconnected components, by definition, do not have edge crossings. Hence, each component is successively considered as current G and partitioned with the solver independently. Suppose the target for the current recursion is Y threads, then the components are partitioned with a target of X threads, chosen as,

$$X = \left\lfloor Y \times \frac{\text{size of the current component}}{\text{size of all components}} \right\rfloor.$$

Heuristic coarsening (S3)

Even with the S1 and S2 techniques, a large graph may have to be two-way partitioned. If the graph is larger than a threshold $thresh_G$, a list-based heuristic coarsening is used before the partitioning. The graph nodes are sorted in a list according to the depth-first traversal order as shown in fig. 8. During the traversal, the differences in depth between subsequent nodes are also noted in a list. The third list indicates the out-degree for each node. The node list is then broken into clusters according to the following criteria:

- The size of the cluster should be less than a *size_threshold*. In the example, cluster 1 is stopped at node 7 for the *size_threshold* of 4.
- The difference in depth among consecutive nodes should be less than a *depth_threshold*. Eg., the difference in depth for the consecutive nodes 7 and 3 is high, so cluster 1 should be stopped at node 7 according to the depth difference as well.
- Clusters should be stopped at the nodes with out-degree higher than a *degree_threshold*. Eg., cluster 2 is stopped at node 6 if the *degree_threshold* is 2.

A coarse graph is constructed with these clusters, which will be used as the current G for two-way partitioning. The clusters are represented as a single node in the coarse graph with a node weight (amount of computation) equal to the sum of all the enclosing node weights. If the resulting graph is very coarse, then it may adversely affect the quality of the subsequent two-way partitioning. The thresholds are chosen according to the current graph size as follows,

$$\begin{aligned} size_threshold &= \frac{\text{size of the current graph to coarsen}}{1000} \\ depth_threshold &= \log_2(size_threshold) \\ degree_threshold &= 10. \end{aligned}$$

With these three techniques, the GRAPHOPT is able to partition graphs with millions of nodes in seconds.

4 PERFORMANCE EVALUATION

To demonstrate the generality of GRAPHOPT, the performance is evaluated for DAGs from two applications: 1) Sparse matrix triangular solves of linear algebra, and 2) Sum-Product Networks of probabilistic machine learning.

4.1 Sparse matrix triangular solves

Matrix triangular solve is a fundamental operation needed to solve linear system of equations $Lx=b$, where L is a lower (or upper) triangular matrix and the vector x is evaluated for a given vector b [16]. This operation has wide-ranging use in engineering simulations, structural analysis, power systems

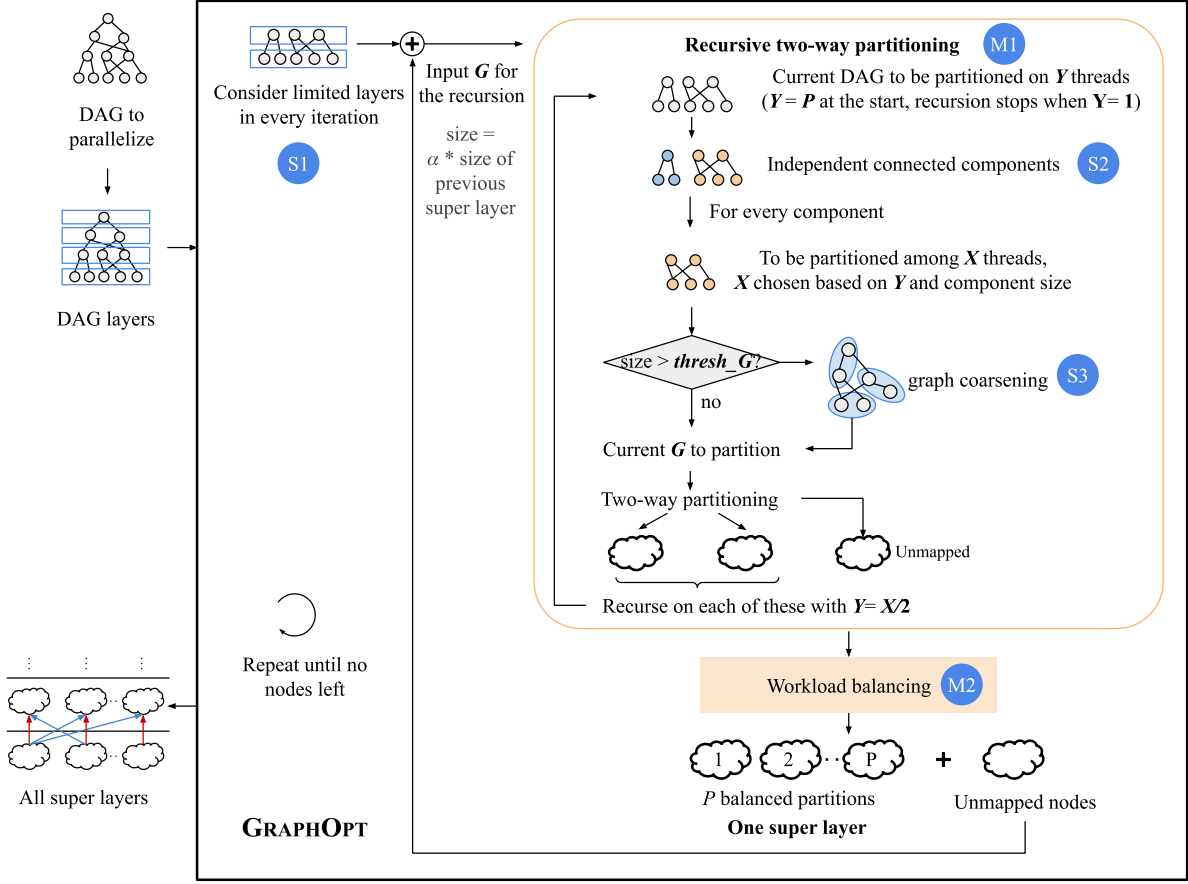


Fig. 7. The full flow with S1, S2, and S3 scalability steps that enables the GRAPHOPT to handle large graphs with millions of nodes/edges.

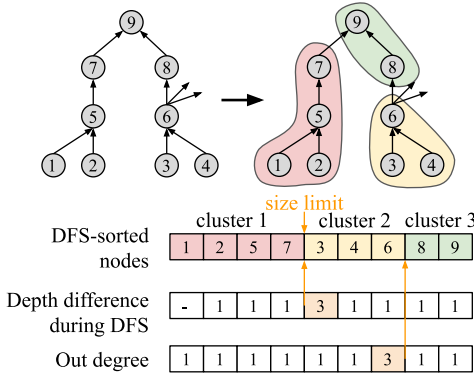


Fig. 8. The data structures generated by depth-first traversal for the heuristic coarsening step (S3)

analysis, economics, control, etc. The matrices arising in real-world problems typically turn out to be sparse, i.e. most of the matrix elements are zero. For example, in electric circuit simulations, a matrix can represent the connectivity of a circuit, with rows/columns indicating the circuit nodes and the matrix elements indicating whether two nodes are connected. Since real-world circuit nodes are typically connected to only a few other nodes, such a connectivity matrix will be sparse. Furthermore, in many applications the sparsity pattern of the matrix remains identical across multiple triangular solves (e.g. the electric circuit structure

may remain the same across simulations), providing the opportunity to perform extensive partitioning to improve the runtime performance.

The computation of the triangular solve can be represented with a DAG, where each node represents the multiply-accumulate (MAC) operations to be performed for each row. If a matrix element $L[i,j]$ is non zero, the DAG contains an edge from node j to node i , indicating the data dependence of triangular solves. The numbers of DAG nodes and edges are the same as the number of rows and non-zero elements in the matrix, respectively. These DAGs are partitioned with GRAPHOPT in our experiments.

Experiments

Several experiments are conducted to evaluate the performance of GRAPHOPT using the matrices from the SparseSuite collection [17] of real-world applications. The super layers generated from the GRAPHOPT are parallelized across multicore CPU threads using OpenMP. The throughput results are averaged over 1000 iterations on a 12 core Intel(R) i5-6500 CPU with GCC v4.8.5 compiler, `-march=native -Ofast` flags, and the thread affinity environment variable set to `KMP_AFFINITY = granularity = fine, compact, 1, 0`. The results are summarized in fig. 9.

| | | | | | | | |
|----|---|-------------|------------|-----------------------|------------------|--------------------|------------------|
| a) | Matrix name | Bai_tols340 | HB_steam1 | Bindel_ted_B_unscaled | Pothen_barth5 | Oberwolfach_gyro_m | Boeing_crystm02 |
| b) | Dimensions | 340x340 | 240x240 | 10605x10605 | 15606x15606 | 17361x17361 | 13965x13965 |
| c) | # non-zeros (density %) | 597 (0.5) | 4120 (7.1) | 94K (0.08) | 478K (0.2) | 752K (0.3) | 2.9M (1.5) |
| d) | Operations in super layers with $P=2$ (blue) and DAG layers (orange) Operations (log scale) vs. super layer idx or DAG layer idx (log scale) | | | | | | |
| e) | Workload balancing for $P=2$ and 8 (Operations vs. super layer idx) super layer=1 is the bottom most super layer | | | | | | |
| f) | Throughput scaling (GFLOPS vs. parallel threads P) | | | | | | |
| g) | Partition time w/o scalability opt. ($P=2$) (sec) | 1.1 | 3.3 | 315.2 | TimeOut (>3600s) | TimeOut (>3600s) | TimeOut (>3600s) |
| h) | Partition time w/ scalability opt. ($P=2$) (sec) | 0.05 | 0.6 | 5.8 | 24.1 | 30.3 | 106 |

Fig. 9. Detailed results for several matrices of varying sizes. Row (d) shows that DAGs can be partitioned into a few, large super layers. It also shows the size of the original DAG layers for comparison. Row (e) shows the workload balancing across threads, in the form of operations in different threads in super layers. Row (f) shows the throughput scaling with parallel threads, demonstrating the advantage of using super layers versus direct DAG-layer partitioning. Rows (g) and (h) show the improvement in partitioning time due to scalability techniques S1, S2, and S3.

4.1.1 How large are the super layers?

GRAPHOPT combines nodes from multiple DAG layers to create large super layers. The row (d) in fig. 9 shows the number of operations in super layers compared to the original DAG layers. GRAPHOPT manages to compress large DAGs with thousands of layers into tens of super layers, reducing the required synchronization barriers.

4.1.2 Workload balancing

Large super layers reduce the number of synchronizations, but good parallel performance demands that the workload is also balanced across threads. The row (e) in fig. 9 shows the number of operations in each super layer for P equals to 2 and 8 threads. As seen, GRAPHOPT balances the workload across parallel partitions in a super layer as much as possible. Also note that the granularity of partitions varies

across different super layers, depending on the available parallelism in the corresponding DAG region.

4.1.3 Throughput scaling

The row (f) shows the scaling of throughput with parallel threads. Different matrices reach peak throughput with different preferred threads depending on the parallelism in the DAGs. For comparison, the throughput of direct “DAG layer partitioning” is shown in the orange curve. In this partitioning, the nodes of a single DAG layer are executed in parallel across threads, and the threads are synchronized after every DAG layer. The super layers achieve better performance because they need fewer synchronizations.

4.1.4 Impact of the scalability techniques

To see the impact of S1 to S3 scalability techniques on the partitioning time, the partitioning is performed with

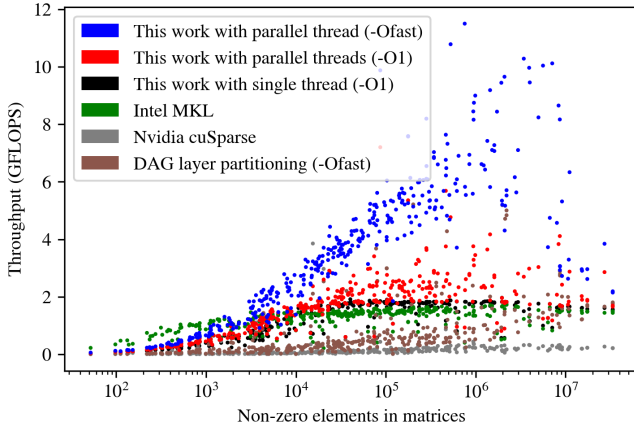


Fig. 10. Throughput comparison with state-of-the-art libraries for triangular solves of 350 matrices

TABLE 2

Mean speedup of this work for 350 matrices compared to baselines

| | Intel MKL | Baseline Nvidia CUSPARSE | DAG layer partitioning |
|--------------------|-----------|--------------------------------|---------------------------|
| This work (-O1) | 1.4× | 23.2× | 6.1× |
| This work (-Ofast) | 3.1× | 42.8× | 11.0× |

and without these techniques, with a timeout of 1 hour. Figure 9(g) and (h) shows that the tool times-out for the larger graphs without these techniques.

4.1.5 Comparison with standard libraries

In this section, the performance of GRAPHOPT is compared with the standard Intel and Nvidia libraries and the standard DAG layer partitioning heuristic, as shown in fig. 10. The performance is evaluated on 350 matrices with varying sizes and non-zero elements from the SparseSuite collection. The caches are *warmed* up by executing the same program before the actual measurement.

Intel MKL: The CPU baseline is evaluated with the standard Intel Math Kernel Library (MKL), which has functions for dense and sparse linear algebra. In particular, the `mkl_sparse_s_trsv()` function is benchmarked with a permission to use all the CPU cores.

Nvidia CUSPARSE: The GPU baseline is evaluated with the Nvidia CUSPARSE library on the RTX 2080Ti GPU. The `cusparsescsrsv_solve()` function is compiled with the CUDA v10.2.89 compiler. The CPU-GPU memory transfers and the CUSPARSE matrix analysis phase are not included in the measurements for a fair comparison.

DAG layer partitioning: This is same as the orange partitioning in the fig. 9, which is a common heuristic approach used in several libraries. The nodes of a DAG layer are executed in parallel across threads (which is possible because, by definition, there are no edges within nodes in a layer), and the threads are synchronized after every layer. The DAG layers are created with the as-late-as-possible (ALAP) heuristic, such that every node is allocated

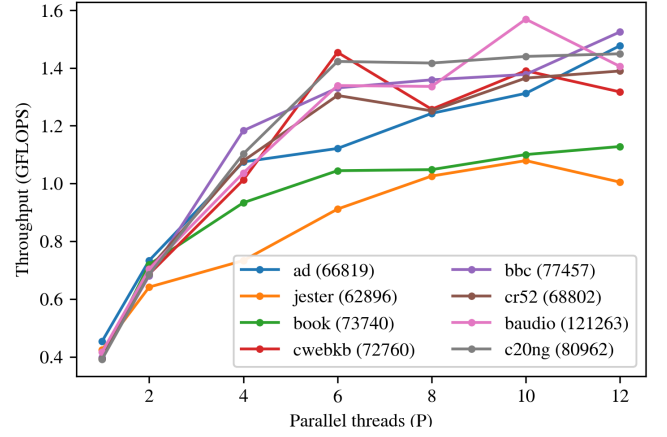


Fig. 11. Throughput scaling for SPNs with increasing parallel threads. The legend shows the name and the number of nodes in the SPNs.

to one layer below its lowest successor node (same as the heuristic used in the S1 technique in section 3.3).

This work: GRAPHOPT is used to generate super layers with P set to 2, 4, ..., 12 parallel threads. **Results:** As shown in fig. 10 the single-threaded performance matches the Intel MKL performance, when compiled with the `-O1` optimization flag. The figure also shows the peak parallel throughput with the `-O1` and `-Ofast` flags. The mean speedup over other techniques are summarized in table 2.

4.2 Sum-Product Networks

The other workload that is used to demonstrate the generality of GRAPHOPT is Sum-Product Network (SPN) [18]. An SPN (more generally called a probabilistic circuit) is a machine learning workload that can tractably model joint probabilities of random variables. SPNs are often used in combination with neural networks, for various reasoning and perceptual tasks like noise-tolerant image recognition [19], robotic navigation [20], robust human-activity detection [21], etc. The SPN is a DAG of sum and product operations that can compute complex probabilistic inferences like the marginal and conditional probability of the random variables. The DAG structure is often irregular and remains unchanged during the inference, making it a good candidate for GRAPHOPT. The experimental setup is the same as the sparse triangular solves. Fig. 11 shows the throughput for 8 SPNs from a standard benchmark [22] with varying parallel threads, achieving a mean speedup of 3.4×

5 RELATED WORK AND DISCUSSION

Sparse triangular solves A common approach for parallelizing triangular solves is the DAG layer partitioning method that partitions nodes on each DAG layer directly into P partitions, and synchronizes the threads after every layer [23], [24], [25], [26]. This is one of the baselines in the experiments section, and is also used in the Nvidia CUSPARSE library [27]. This partitioning is quicker than our approach when the sparsity pattern/DAG structure changes for every triangular solve. However, for large matrices, thousands of

synchronizing barriers might be needed depending on the critical path length of the DAG, incurring large overhead. As shown in our experiments, unnecessary barriers can be avoided by combining multiple DAG layers into super layers, improving the throughput significantly compared to the DAG layer partitioning (table 2).

Another approach is the self-scheduling method, which avoids both, the global barriers and DAG partitioning, for GPU execution [28], [29]. The DAG nodes are executed as individual tasks, and the latency of task launching is minimized by dispatching them at once. The tasks then actively wait (in spin loops) until all the predecessor tasks finish and the required data is available, creating a domino-like self-scheduling effect. However, this active waiting not only consumes compute cycles but can also create significant memory contention. This overhead is exacerbated in large graphs which can have thousands of tasks actively waiting. Furthermore, this approach might be suitable for GPU, which supports low-overhead hardware-enabled thread switching. But the high-overhead thread switching in CPU makes this approach infeasible. Experiments in [30] show that the self-scheduling performs worse than the simple DAG layer partitioning even in GPU.

The works in [31] and [30] are the most similar to this paper, with two key differences:

- 1) Both the papers limits the partition sizes. In [31], the partitions should fit in the local scratchpads of GPU, while in [30], the size is controlled with a predefined hyperparameter that has to be tuned for every DAG. This hyperparameter remains same for the entire DAG even when the local parallelism can vary in different parts of the DAG. This is in contrast with our approach of making the partitions as large as possible as long as there are P parallel partitions to keep the hardware busy. In other words, by explicitly defining the hardware parallelism (via P), GRAPHOPT automatically adjust the partition size based on the available parallelism in the DAG, reducing the overall number of partitions and global barriers.

This partition size limit is unnecessary because a global barrier is not needed when partition sizes, e.g., exceed the GPU scratchpad size. Instead, large partitions can be further divided in subpartitions that fit into the scratchpad, and a local barrier (eg. `__syncthreads()` in CUDA) can be used.

- 2) Both [31] and [30] develop a partitioning heuristic, while GRAPHOPT uses constrained optimization and leverages a state-of-the-art solver, which often achieve better solutions than custom heuristics.

Sum-Product Networks The DAG layer partitioning heuristic is used for SPN for CPU, GPU and a custom ASIC parallelization [32], [33], [34]. Libraries based on Tensorflow have also been developed for coarse-grained SPNs with explicit regular structures [35], [36]. However, such a Tensorflow-based approach is not useful for fine-grained, irregular SPNs due to the overheads of kernel launch etc. GRAPHOPT does not assume any regularity in SPN structure, and can still achieve $3.4\times$ average speedup.

Graph partitioning As explained in section 3, GRAPHOPT

essentially needs to solve P -way independent partitioning of a directed graph while ensuring that resulting partitions are acyclic and balanced. In general, graph partitioning of arbitrary graphs is known to be NP-complete [8], [9] and is a widely studied problem. Several partitioning algorithms have been developed [37], [38], [39], [40], [41], [42], but they only focus on undirected graphs intending to reduce the edge crossings within balanced partitions, while ignoring the edge direction. As a result, the popular undirected partitioning software like JOSTLE [43] and METIS [9] cannot be used for acyclic partitioning.

The acyclic partitioning of DAGs is also shown to be NP-complete like the undirected version of the problem [10]. In recent years, several works have been proposed to tackle the problem [10], [44], [45], [46]. However, these works do not focus on parallelism. The resulting partitions would be acyclic, well-balanced, with minimal edge crossings, but can end up being completely sequential, i.e. only one partition can be executed at a time. This stems from the fact that the usual objective of minimizing edge crossings does not guarantee parallelism. Hence, these methods are not suitable for parallelizing a DAG execution over multiple threads.

Several runtime and compile-time algorithms have been proposed for scheduling DAGs [47], [48], [49], [50], [51], [52], [53], [54], [55], [56], which use either list-based or clustering-based scheduling heuristics, while GRAPHOPT takes a different approach of modeling the core routine of the tool as a constrained-optimization problem, allowing the use of open-source solvers. Such a constrained optimization-based approach is also explored in [57], [58]. However, these works could only handle tens of DAG nodes, which is completely insufficient for real-world workloads. The reason for this inscalability is that they attempt to find the globally optimal schedule for the entire DAG by modeling it as a single optimization problem. This becomes intractable for larger DAGs even with their simplifying assumptions. GRAPHOPT contributes by making the large graph partitioning feasible with scalability heuristics.

Suggestions for future work The two-way partitioning model in section 3.1 can be extended to P -way partitions by simply allowing the *PART* variable to take values in integers $[0, P]$ instead of $[0, 2]$. This would find P partitions of a super layer directly, avoiding recursive two-way partitioning. However, allowing values in $[0, P]$ adds symmetries in the search space since two partitions can be switched without breaking any constraint. These symmetries prohibitively increase the run time of the solver since it keeps finding (or refuting) candidates that are just permutations of an earlier solution (or non-solution). The usual technique of symmetry breaking using lexicographical ordering constraint on the *PART* variable is not sufficient because it does not break all the symmetries. A recent paper [59] proposes stricter symmetry breaking constraints for several graph optimization problems, which we believe can also be applied to this problem. We leave this as a future improvement to this work.

6 CONCLUSION

This paper describes GRAPHOPT, a tool developed to efficiently parallelize sparse, irregular graph workloads on parallel compute threads. Graphs are decomposed into super layers with P parallel partitions, using multiple recursions of two-way partitioning of subgraphs. The two-way partitioning problem is modeled as an optimization problem with the Minizinc constraint-modeling language and solved with the open Google OR-Tools solver. The full flow of GRAPHOPT also contains steps for workload balancing and scalability techniques to handle large graphs. The resulting performance of this super layer-based partitioning is benchmarked for sparse matrix triangular solves and sum-product networks. Multiple experiments are performed with widely varying sizes of matrices to show the different aspects of the tool. GRAPHOPT achieves $1.4\times$, $1.4\times$, $23.2\times$, and $6.1\times$ mean speedup over the single-threaded execution, Intel MKL, Nvidia CUSPARSE library, and the DAG layer partitioning heuristic, respectively. Thus, GRAPHOPT demonstrates that constrained optimization is effective for the parallelization of large graph workloads.

REFERENCES

- [1] M. Abadi, P. Barham, J. Chen, Z. Chen, A. Davis, J. Dean, M. Devin, S. Ghemawat, G. Irving, M. Isard, M. Kudlur, J. Levenberg, R. Monga, S. Moore, D. G. Murray, B. Steiner, P. Tucker, V. Vasudevan, P. Warden, M. Wicke, Y. Yu, and X. Zheng, "Tensorflow: A system for large-scale machine learning," in *12th USENIX Symposium on Operating Systems Design and Implementation (OSDI 16)*, 2016, pp. 265–283.
- [2] J. Ragan-Kelley, C. Barnes, A. Adams, S. Paris, F. Durand, and S. P. Amarasinghe, "Halide: a language and compiler for optimizing parallelism, locality, and recomputation in image processing pipelines," in *ACM SIGPLAN Conference on Programming Language Design and Implementation, PLDI*, 2013, pp. 519–530.
- [3] B. Pradelle, B. Meister, M. M. Baskaran, J. Springer, and R. Lethin, "Polyhedral optimization of tensorflow computation graphs," in *Programming and Performance Visualization Tools*, vol. 11027, 2017, pp. 74–89.
- [4] T. Huang, C. Lin, G. Guo, and M. D. F. Wong, "Cpp-taskflow: Fast task-based parallel programming using modern C++," in *2019 IEEE International Parallel and Distributed Processing Symposium, IPDPS*, 2019, pp. 974–983.
- [5] A. D. Robison, *Intel® Threading Building Blocks (TBB)*, 2011, pp. 955–964. [Online]. Available: https://doi.org/10.1007/978-0-387-09766-4_51
- [6] S. Puthoor, A. M. Aji, S. Che, M. Daga, W. Wu, B. M. Beckmann, and G. Rodgers, "Implementing directed acyclic graphs with the heterogeneous system architecture," in *Proceedings of the 9th Annual Workshop on General Purpose Processing using Graphics Processing Unit*, 2016, pp. 53–62.
- [7] T. Gautier, J. V. F. Lima, N. Maillard, and B. Raffin, "Xkaapi: A runtime system for data-flow task programming on heterogeneous architectures," in *27th IEEE International Symposium on Parallel and Distributed Processing, IPDPS*, 2013, pp. 1299–1308.
- [8] A. E. Feldmann, "Fast balanced partitioning is hard even on grids and trees," *Theoretical Computer Science*, vol. 485, pp. 61–68, 2013.
- [9] G. Karypis and V. Kumar, "A fast and high quality multilevel scheme for partitioning irregular graphs," *SIAM Journal on scientific Computing*, vol. 20, no. 1, pp. 359–392, 1998.
- [10] O. Moreira, M. Popp, and C. Schulz, "Evolutionary multi-level acyclic graph partitioning," *Journal of Heuristics*, vol. 26, no. 5, pp. 771–799, 2020.
- [11] L. Perron and V. Furnon, "Or-tools," Google. [Online]. Available: <https://developers.google.com/optimization/>
- [12] N. Nethercote, P. J. Stuckey, R. Becket, S. Brand, G. J. Duck, and G. Tack, "Minizinc: Towards a standard CP modelling language," in *Principles and Practice of Constraint Programming - CP*, vol. 4741, 2007, pp. 529–543.
- [13] G. Gamrath, D. Anderson, K. Bestuzheva, W.-K. Chen, L. Eifler, M. Gasse, P. Gemander, A. Gleixner, L. Gottwald, K. Halbig, G. Hendel, C. Hojny, T. Koch, P. Le Bodic, S. J. Maher, F. Matter, M. Miltenberger, E. Mühmer, B. Müller, M. E. Pfetsch, F. Schlösser, F. Serrano, Y. Shinano, C. Tawfik, S. Vigerske, F. Wegscheider, D. Weninger, and J. Witzig, "The SCIP Optimization Suite 7.0," Optimization Online, Technical Report, March 2020.
- [14] Gurobi Optimization LLC, "Gurobi optimizer reference manual," 2021. [Online]. Available: <http://www.gurobi.com>
- [15] T. Nowatzki, M. C. Ferris, K. Sankaralingam, C. Estan, N. Vaish, and D. A. Wood, *Optimization and Mathematical Modeling in Computer Architecture*, ser. Synthesis Lectures on Computer Architecture, 2013.
- [16] T. A. Davis, S. Rajamanickam, and W. M. Sid-Lakhdar, "A survey of direct methods for sparse linear systems," *Acta Numer.*, vol. 25, pp. 383–566, 2016.
- [17] T. A. Davis and Y. Hu, "The university of florida sparse matrix collection," *ACM Transactions on Mathematical Software (TOMS)*, vol. 38, no. 1, pp. 1:1–1:25, 2011.
- [18] R. Sanchez-Cauce, I. Paris, and F. J. Diez Vegas, "Sum-product networks: A survey," *IEEE Transactions on Pattern Analysis and Machine Intelligence*, pp. 1–1, 2021.
- [19] K. Stelzner, R. Peharz, and K. Kersting, "Faster attend-infer-repeat with tractable probabilistic models," in *Proceedings of the 36th International Conference on Machine Learning, ICML*, vol. 97, 2019, pp. 5966–5975.
- [20] K. Zheng and A. Pronobis, "From pixels to buildings: End-to-end probabilistic deep networks for large-scale semantic mapping," in *2019 IEEE/RSJ International Conference on Intelligent Robots and Systems (IROS)*, 2019, pp. 3511–3518.
- [21] L. I. G. Olascoaga, W. Meert, N. Shah, M. Verhelst, and G. V. den Broeck, "Towards hardware-aware tractable learning of probabilistic models," in *Advances in Neural Information Processing Systems (NeurIPS)*, 2019, pp. 13726–13736.
- [22] Y. Liang, J. Bekker, and G. V. den Broeck, "Learning the structure of probabilistic sentential decision diagrams," in *Proceedings of the Thirty-Third Conference on Uncertainty in Artificial Intelligence UAI*, 2017.
- [23] B. Yilmaz, B. Sipahioğlu, N. Ahmad, and D. Unat, "Adaptive level binning: A new algorithm for solving sparse triangular systems," 2020, p. 188–198.
- [24] E. Anderson and Y. Saad, "Solving sparse triangular linear systems on parallel computers," *International Journal of High Speed Computing*, vol. 1, no. 1, pp. 73–95, 1989.
- [25] E. Dufrechou and P. Ezzatti, "A new GPU algorithm to compute a level set-based analysis for the parallel solution of sparse triangular systems," in *2018 IEEE International Parallel and Distributed Processing Symposium (IPDPS)*, 2018, pp. 920–929.
- [26] R. Li and Y. Saad, "Gpu-accelerated preconditioned iterative linear solvers," *The Journal of Supercomputing*, vol. 63, no. 2, pp. 443–466, 2013.
- [27] M. Naumov, "Parallel solution of sparse triangular linear systems in the preconditioned iterative methods on the gpu," *NVIDIA Corp., Westford, MA, USA, Tech. Rep. NVR-2011*, vol. 1, 2011.
- [28] W. Liu, A. Li, J. D. Hogg, I. S. Duff, and B. Vinter, "Fast synchronization-free algorithms for parallel sparse triangular solves with multiple right-hand sides," *Concurrency and Computation: Practice and Experience*, vol. 29, no. 21, 2017.
- [29] J. I. Aliaga, E. Dufrechou, P. Ezzatti, and E. S. Quintana-Ortí, "Accelerating the task/data-parallel version of ilupack's bicg in multi-cpu/gpu configurations," *Parallel Computing*, vol. 85, pp. 79–87, 2019.
- [30] A. E. Helal, A. M. Aji, M. L. Chu, B. M. Beckmann, and W. Feng, "Adaptive task aggregation for high-performance sparse solvers on gpus," in *28th International Conference on Parallel Architectures and Compilation Techniques PACT*, 2019, pp. 324–336.
- [31] A. Picciau, G. E. Inggs, J. Wickerson, E. C. Kerrigan, and G. A. Constantinides, "Balancing locality and concurrency: Solving sparse triangular systems on gpus," in *23rd IEEE International Conference on High Performance Computing HiPC*, 2016, pp. 183–192.
- [32] M. Dang, P. Khosravi, Y. Liang, A. Vergari, and G. Van den Broeck, "Juice: A julia package for logic and probabilistic circuits," in *Proceedings of the 35th AAAI Conference on Artificial Intelligence (Demo Track)*, 2021.
- [33] N. Shah, L. I. G. Olascoaga, W. Meert, and M. Verhelst, "Acceleration of probabilistic reasoning through custom processor archi-

- ecture," in *2020 Design, Automation & Test in Europe Conference & Exhibition DATE*, 2020, pp. 322–325.
- [34] V. Dadu, J. Weng, S. Liu, and T. Nowatzki, "Towards general-purpose acceleration: Finding structure in irregularity," *IEEE Micro*, vol. 40, no. 3, pp. 37–46, 2020.
- [35] A. Pronobis and R. P. N. Rao, "Learning deep generative spatial models for mobile robots," in *2017 IEEE/RSJ International Conference on Intelligent Robots and Systems IROS*, 2017, pp. 755–762.
- [36] A. Molina, A. Vergari, K. Stelzner, R. Peharz, P. Subramani, N. D. Mauro, P. Poupart, and K. Kersting, "SPFlow: An easy and extensible library for deep probabilistic learning using sum-product networks," 2019.
- [37] G. M. Slota, C. Root, K. Devine, K. Madduri, and S. Rajamanickam, "Scalable, multi-constraint, complex-objective graph partitioning," *IEEE Transactions on Parallel and Distributed Systems*, vol. 31, no. 12, pp. 2789–2801, 2020.
- [38] A. Buluç, H. Meyerhenke, I. Safro, P. Sanders, and C. Schulz, "Recent advances in graph partitioning," in *Algorithm Engineering - Selected Results and Surveys*, 2016, vol. 9220, pp. 117–158.
- [39] D. LaSalle, M. M. A. Patwary, N. Satish, N. Sundaram, P. Dubey, and G. Karypis, "Improving graph partitioning for modern graphs and architectures," in *Proceedings of the 5th Workshop on Irregular Applications - Architectures and Algorithms IA3*, 2015, pp. 14:1–14:4.
- [40] C.-E. Bichot and P. Siarry, *Graph partitioning*. John Wiley & Sons, 2013.
- [41] C. Aykanat, B. B. Cambazoglu, and B. Uçar, "Multi-level direct k-way hypergraph partitioning with multiple constraints and fixed vertices," *Journal of Parallel and Distributed Computing*, vol. 68, no. 5, pp. 609–625, 2008.
- [42] K. D. Devine, E. G. Boman, and G. Karypis, "Partitioning and load balancing for emerging parallel applications and architectures," in *SIAM Parallel Processing for Scientific Computing*, 2006, vol. 20, pp. 99–126.
- [43] C. Walshaw and M. Cross, "Jostle: parallel multilevel graph-partitioning software—an overview," *Mesh partitioning techniques and domain decomposition techniques*, vol. 10, 2007.
- [44] J. Herrmann, M. Y. Özkaya, B. Uçar, K. Kaya, and Ü. V. Çatalyürek, "Multilevel algorithms for acyclic partitioning of directed acyclic graphs," *SIAM Journal of Scientific Computing*, vol. 41, no. 4, pp. A2117–A2145, 2019.
- [45] O. Moreira, M. Popp, and C. Schulz, "Graph partitioning with acyclicity constraints," in *16th International Symposium on Experimental Algorithms SEA*, vol. 75, 2017, pp. 30:1–30:15.
- [46] J. Cong, Z. Li, and R. L. Bagrodia, "Acyclic multi-way partitioning of boolean networks," in *Proceedings of the 31st Conference on Design Automation*. ACM Press, 1994, pp. 670–675.
- [47] B. Bramas and A. Ketterlin, "Improving parallel executions by increasing task granularity in task-based runtime systems using acyclic DAG clustering," *PeerJ Computer Science*, vol. 6, p. e247, 2020.
- [48] M. Y. Özkaya, A. Benoit, B. Uçar, J. Herrmann, and Ü. V. Çatalyürek, "A scalable clustering-based task scheduler for homogeneous processors using DAG partitioning," in *2019 IEEE International Parallel and Distributed Processing Symposium, IPDPS*, 2019, pp. 155–165.
- [49] H. Wang and O. Sinnen, "List-scheduling versus cluster-scheduling," *IEEE Transactions on Parallel and Distributed Systems*, vol. 29, no. 8, pp. 1736–1749, 2018.
- [50] H. Kanemitsu, M. Hanada, and H. Nakazato, "Clustering-based task scheduling in a large number of heterogeneous processors," *IEEE Transactions on Parallel and Distributed Systems*, vol. 27, no. 11, pp. 3144–3157, 2016.
- [51] H. Arabnejad and J. G. Barbosa, "List scheduling algorithm for heterogeneous systems by an optimistic cost table," *IEEE Transactions on Parallel and Distributed Systems*, vol. 25, no. 3, pp. 682–694, 2014.
- [52] L. F. Bittencourt, R. Sakellariou, and E. R. M. Madeira, "Dag scheduling using a lookahead variant of the heterogeneous earliest finish time algorithm," in *2010 18th Euromicro Conference on Parallel, Distributed and Network-based Processing*, 2010, pp. 27–34.
- [53] V. Sarkar, *Partitioning and Scheduling Parallel Programs for Multiprocessors*. Cambridge, MA, USA: MIT Press, 1989.
- [54] C. Rossignon, P. Hénon, O. Aumage, and S. Thibault, "A numa-aware fine grain parallelization framework for multi-core architecture," in *2013 IEEE International Symposium on Parallel Distributed Processing, Workshops and Phd Forum*, 2013, pp. 1381–1390.
- [55] H. Topcuoglu, S. Hariri, and Min-You Wu, "Performance-effective and low-complexity task scheduling for heterogeneous computing," *IEEE Transactions on Parallel and Distributed Systems*, vol. 13, no. 3, pp. 260–274, 2002.
- [56] R. Mayer, C. Mayer, and L. Laich, "The tensorflow partitioning and scheduling problem: It's the critical path!" in *Proceedings of the 1st Workshop on Distributed Infrastructures for Deep Learning*, 2017, p. 1–6.
- [57] C. Valouxis, C. Gogos, P. Alefragis, G. Goulas, N. Voros, and E. Housos, "Dag scheduling using integer programming in heterogeneous parallel execution environments," in *Proceedings of the Multidisciplinary International Conference on Scheduling: Theory and Applications MISTA*, 2013, pp. 392–401.
- [58] G. Goulas, C. Gogos, C. Valouxis, P. Alefragis, and N. S. Voros, "Coarse grain parallelization using integer programming," in *2013 11th IEEE International Conference on Industrial Informatics (INDIN)*, 2013, pp. 816–820.
- [59] M. Codish, A. Miller, P. Prosser, and P. J. Stuckey, "Constraints for symmetry breaking in graph representation," *Constraints*, vol. 24, no. 1, pp. 1–24, 2019.